Structural, Morphological and Supercapacitor Performance of Reduced Graphene Oxide Nanomaterials for Future Generation Energy Storage Devices

D.Govindarajan[1]*, M.Joseph Salethraj[1]
[1]Department of Physics, Annamalai University, Annamalai Nagar - 608 002, India
Corresponding author: degerajan@gmail.com.

Abstract

In this work, The Reduced Graphene oxide (RGO) was prepared from the pure Graphite powder by using modified Hummer's method. The synthesized RGO was characterized through X-ray diffraction (XRD), Fourier transform infra-red spectroscopy(FTIR), Micro-Raman, Scanning electron microscopy(SEM), high resolution transmission electron microscopy(HRTEM) with EDX and Cyclic Voltammetric studies. The XRD characteristic peak of graphene oxide (GO) appeared at 11.89˚ and the RGO characteristic peak spotted at 24.06˚. The functional group analysis of RGO was carried out by FTIR spectroscopy. The Raman characteristic peak of RGO appeared at 1338 $cm^{-1}$and 1590 cm^{-1} which implies that the D band and G band of Sp^2 carbon material. The SEM and HRTEM images of GO and RGO appeared as a layered nanosheet shapes. The EDX spectrum of RGO shows only carbon and oxygen element which indicates the purity of the RGO. The CV results of the RGO electrode exhibit a typical rectangular shape with good specific capacitance valueof 94 Fg^{-1}@10 mvS^{-1}.

Key words: Reduced Graphene Oxide; SEM;HRTEM; Cyclic Voltammetric.

DOI Number: 10.48047/NQ.2022.20.16.NQ880478 Neuroquantology 2022; 20(16): 4685-4694

1. Introduction

Now days increasing the necessity of energy demand, the researchers are focusing on the renewable and sustainable energy storage materials [1]. For the last ten years, graphene based materials have much more attraction for the researchers due to its unique arrangement of Sp^2bonded carbon atom with the planer sheet and honeycomb crystal lattice [2]. Due to the physical and chemical properties, it has beenapplied in different areas like adsorbents, catalyst, and thermal transporter, electrode materials in Supercapacitors (SCs), batteries and sensors. Among them, the electrochemical storage devices have much more attention in the present scenario. Because, it has wide range of benefits than the conventional energy storages due to its energy density, power density and the cyclic stability. In SC, the energy is stored either in the terms of electric double layer [EDLC] (carbon based materials) or pseudocapacitance (metal oxides or conducting

polymers). For SC applications various electrode nanomaterials are utilized by the researchers to achieve higher energy density and power density. Currently the researchers more attention to prepare and used graphene oxide as an electrode material for energy storage devices. Since the GO areformed as layered sheets and synthesized from graphite powder, which is inexpensive and available in huge quantities.Naturally graphene oxide sheet have the outstanding property of theoretical surface area, good electrical and thermal stability, chemical tolerance and broad electrochemical window[3].

In this work, the graphene oxide was derived from graphite powder using themodified Hummer's method. Finally, the obtained GO nanoparticles (NPs)are reduced and are characterzed through XRD, FTIR, Raman, SEM and TEM studies. The RGO nanoparticles are utilized for electrode materials to analyze for CV studies.

2. Experimental Section

2.1 Materials

For the preparation of RGO, the following analytical grade of chemicals was purchased from Merck India Pvt. Ltd. with a purity of 99%. Graphite powder,potassium permanganate, sodium nitrate, hydrogen peroxide (H_2O_2), sulfuric acid, hydrochloric acid, hydrazine hydrate (N_2H_4), polyvinylidene difluoride (PVDF), *N*-methyl-2-pyrrolidone (NMP) and acetylene black.

2.2 Synthesis of Graphene oxide and Reduced Graphene oxide

1g of graphite powder and 1g of sodium nitrate were dissolved in 50ml of sulfuric acid and the reaction was carried out in an ice water bath. Then 6g of potassium permanganate were added slowly with the above mixture and stirred for 5 hr. After that, the beaker was taken out from the ice water bath and continues the reaction at 80˚C temperature.Then 100ml of DI water was added and stirred for 3hrs. Finally, 50 ml of hydrogen peroxide was added until mixture was turned into yellowish green from dark brown colour. The obtained GO powder was washed with DI water and ethanol for several times. The GO powder was reduced to RGO by stirredwith the addition ofhydrazine hydrate.

2.3 Characterization techniques:

The XRD spectrum were record in PAN analytical X'Pert PRO powder X-ray diffractometer recorded in the range of 10°to 80° with the monochromatic radiation Cu Kα radiation (λ = 1.54060 Å). Functional groupanalysis of RGO isanalyzed byPerkin Elmer make FTIR Spectrometer (Model - RXI).LABRAM HR instrument was used to record Micro Raman spectrum of RGO with source as 633 nm laser excitation. SEM and TEM with EDXimages were taken in ZEISS instrument and FEI-TECNAI G2-20 S-TWIN HRTEM, respectively.

2.4 Electrochemical Measurement:

The electrochemical analysis of RGO electrode was carried out by Biologic SP-300 electrochemical workstation. In the present study,Ag/AgCl electrode was used as a reference electrode and platinum wireas a counter electrode. The working electrode was fabricated by grinding of RGO with PVDF and acetylene black in 80:10:10ratio andNMP used as a wetting and binding agent. After fine mixing, the slurry was coated on nickel plate (1 cm X 1 cm) and dried at 120°C for 12h. The cyclic voltammetric curve of the RGO electrode was recorded in KOH electrolyte solution with the potential window varied from 0V to 1V in a three electrode system.

3. Result and Discussion

3.1. XRD analysis

Figure 1 shows XRD spectrum of synthesized GO and RGO NPs. From the XRD

spectrum of GO (Figure 1(a)), a strong peak observed at 11.89° is related to (002) plane which is the characteristic peak of GO [10]. The corresponding d spacing value of GO is 0.74 nm.A small hump appear at 42.02˚ may be due to turbostatic disorder of GO sheet [4]

From the RGO XRD spectra (Figure 1(b)), the characteristicGOpeak (11.89˚) is totally vanishedand the new peak observed at 24.06˚ indicating the RGO formation. Also the d spacing value of RGO as 0.31 nm indicating the successful reduction of GOfrom the graphitic structures. As compared to GO, the decrement in d spacing value indicates the interlayer reduction of GO, elimination water and oxygen containing groups. The broad hump in the spectra indicates the graphene flakes are randomly oriented in the stacking direction [5].

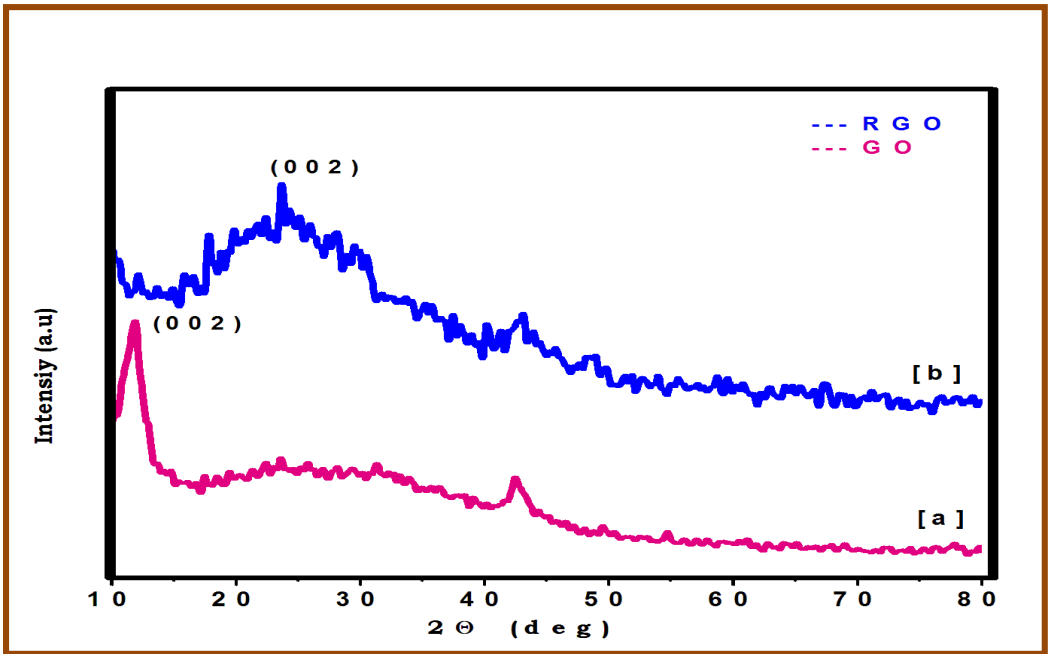

Figure1: XRD Spectrum of (a) GO and (b) RGO NPs.

3.2. FTIR Analysis

FTIR is a potential tool to analysis the functional groups of synthesized RGO NPs and the spectra was recorded from 4000 cm^{-1} to 400 cm^{-1} (Figure 2). A wide peak arise at 3414 cm^{-1} which denote the OH (hydroxyl) group and this may due to the intercalation water molecules in GO. A minor peak spotted at 2930 cm^{-1}isdue to CH_2 stretching vibration of RGO [6]. The strong peak appeared at 1610 cm^{-1} is attributed to the bending vibration of surface absorbed H_2O molecules as well as the contribution of Sp^2 bond [7]. The peak at 1410 cm^{-1} arises due to the deformation of O-H vibration. The C-O peak appears at 1050 cm^{-1} which strongly denotes the well formation of RGO [8].

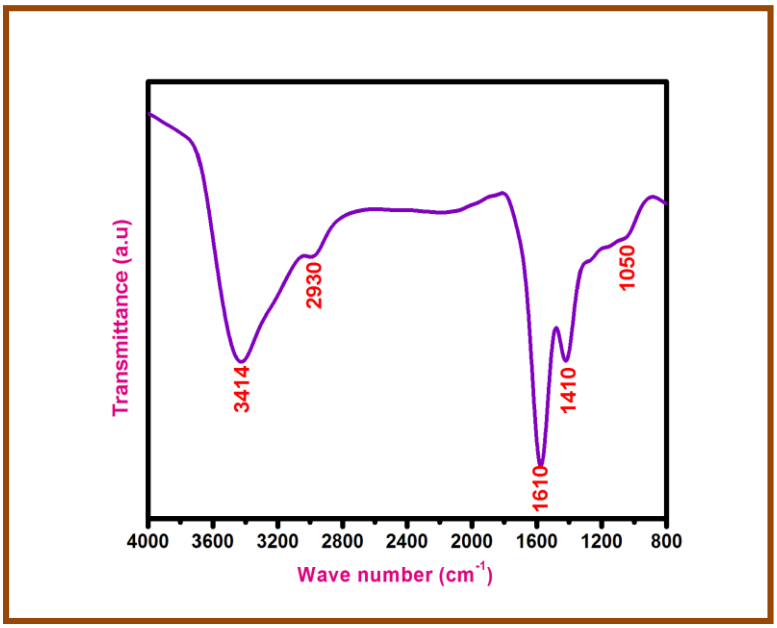

Figure 2: FTIR Spectrum of RGO NPs.

3.3. Micro Raman Analysis

The Micro Raman is spectrum used to analysis the chemical, structural and vibrational bands of GO (Figure3)and RGO (Figure 4).From the figure, two strong peaks are noted at 1338 cm^{-1} and 1590 cm^{-1} denotes the D (defect) band and G (graphitic) band, respectively. The D band arises due to the stretching vibration of Sp^3 carbon,which is related to the order/disorder of the system. Also, the G bandmainly caused by the stretching vibrations of Sp^2 carbon atoms and it is related with the first order scattering of the E_{2g} mode. In GO spectrum, the intensity of G band is slightly greater than the D band denoting the formation of GO from graphite where as in RGO spectrum the intensity of D band is higher than G indicating the structural imperfection by the attachment of functional groups in the plane of graphene sheet [9].The intensity ratio of these band value (I_D/I_G) helps to identify the number of layers in graphene and also the overall stacking behavior. The I_D/I_Gratio is calculated for GO as83 % and RGO as 92%, which indicates the higher degree of exfoliation/disorder of the graphene material [10].

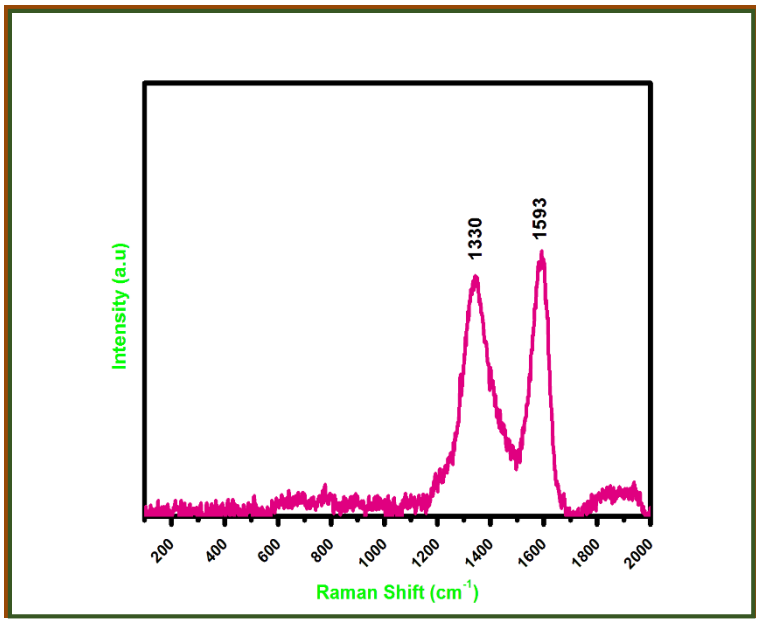

Figure 3: Micro Raman Spectrum of GO NPs.

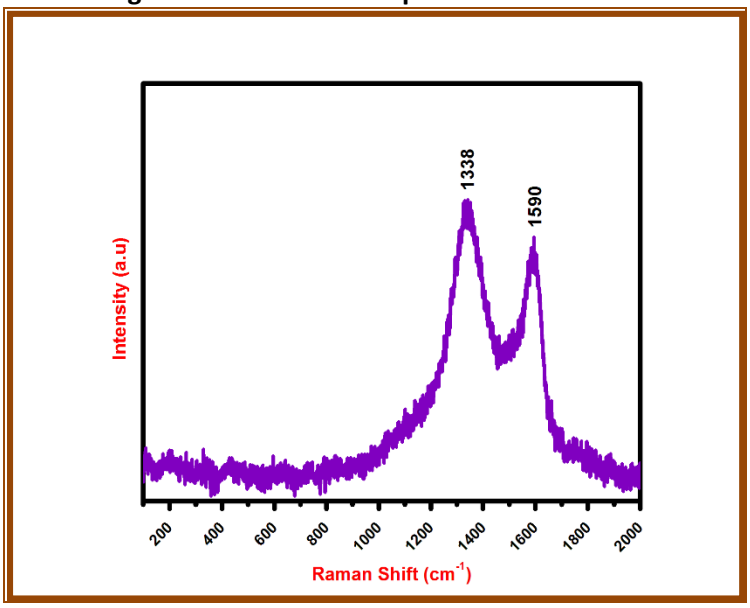

Figure4: Micro Raman Spectrum of RGO NPs.

3.4. Morphology analysis

Figure 5(a) & (b) shows the SEM images of RGO and it portraits the wrinkled andcrumbled surface of RGO nanosheets, which arise due to breaking and deformation of Sp^2 carbon bond from GO. The HRTEM images (Figure 5(c) & (d)) clearly show that the RGO appear as large transparent wavy nanosheetswith soft edge. The higher transparencies of the RGO nanosheets suggest that more number ofmonolayer in the graphene network. Also, wrinkled nature of the RGO nanosheet increases the surface area, which may promote more ion interaction between electrode and electrolyte in CV studies [11]. Figure5(e) Represent the SAED pattern of RGO nanosheet, where the diffraction rings clearly indicate the (002) plane of RGO and well

matched with XRD results. The carbon and oxygen peaks only spotted on the EDX spectrum (Figure 5(f)), which reveals the purity of the synthesized RGO nanomaterial.

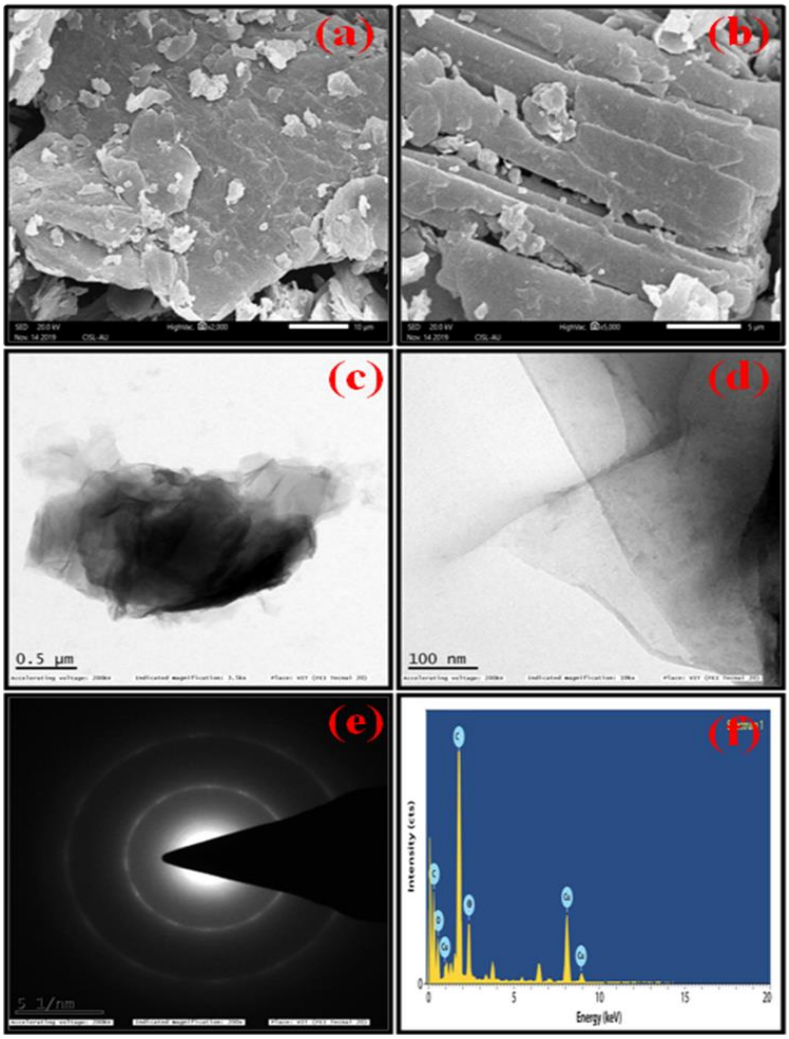

Figure 5:(a)&(b) SEM images, (c)&(d) HRTEM images, (e) SAED pattern, (f) EDX spectrum of RGO NPs.

3.5. Electrochemical analysis

The electrochemical analysis was carried out in electrochemical workstation in 1M KOH used as an electrolyte solution. Figure 6 shows the CV cure of RGO NPs at various scan rates
(10 mVs^{-1}, 30 mVs^{-1}, 50 mVs^{-1}, 70 mVs^{-1} and 100 mVs^{-1}) with the potential window (0V to 1V).

From the Figure 6, the CV curve of RGO portrait the quasi-rectangular shape which indicates the RGO electrode behaves like an ideal EDLC nature [12-17].The specific capacitance of the RGO electrode was calculated by the following equation [17, 18] and the values are shown in table 1.

$$C_p = \frac{A}{m\Delta V} \quad \ldots (1)$$

eISSN1303-5150

Where A - representthe active surface area, m - represent the mass of the sample and ΔV - representthe scan rate. Figure 7 shows the specific capacitance of RGO electrode. From the Figure 7, it is noted that the RGO electrode exhibit good specific capacitance value of 94 F/g at the scan rate of 10 mVs^{-1}.At lower scan rate, the ion gets more time to absorption and diffusion of the electrode so that it exhibit good specific capacitance. Whereas the scan rate increases, the specific capacitance value of RGO was decreased to 31 F/g, due to the short time of ion diffusion and absorption with the electrode material and electrolyte.

Table 1: Specific capacitance values of RGO electrode

Scan rate (mV S^{-1})	Specific Capacitance (Fg^{-1})
10	94
30	65
50	43
70	37
100	31

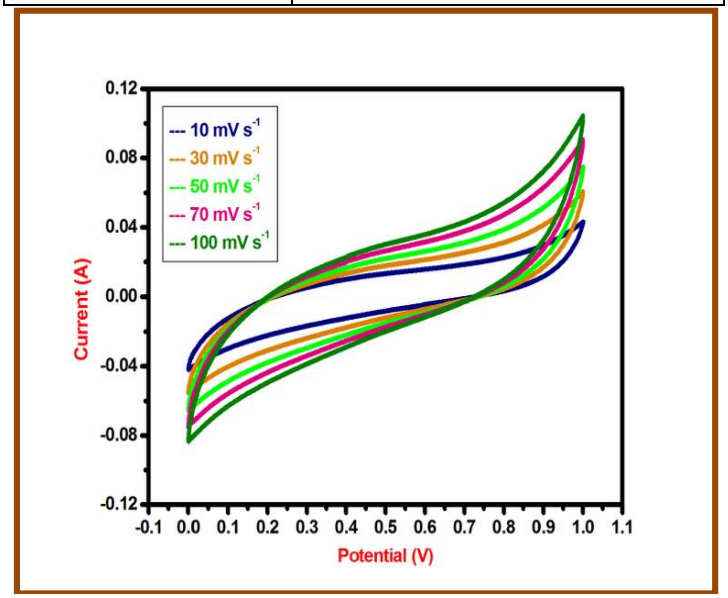

Fig. 6: CV curve of RGO electrode.

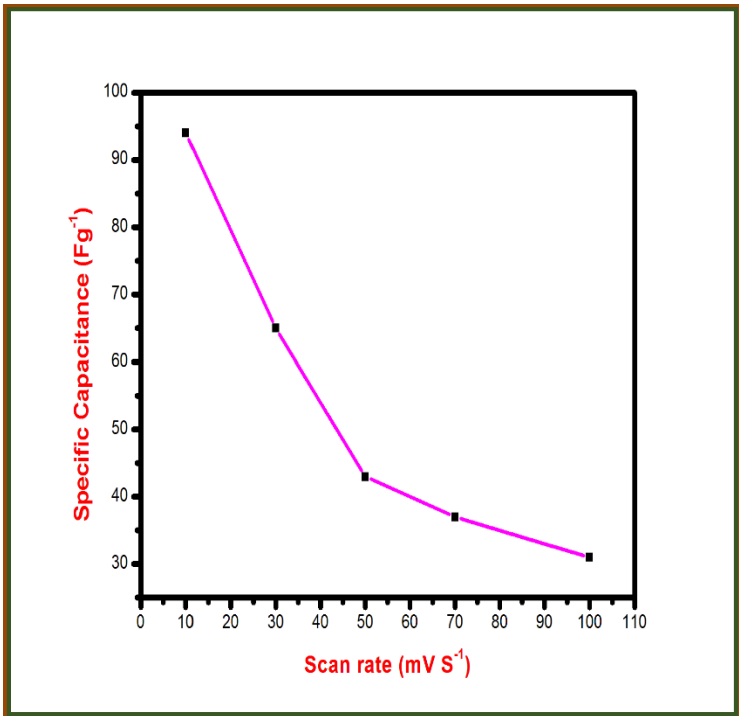

Fig. 7: Specific capacitance (vs) Scan rate of RGO electrode.

Conclusion:

The RGO was successfully synthesized by modified Hummer's method. The structural, morphological and compositional properties of RGO were studied through XRD, SEM and TEM with EDAX studies. The prepared RGO electrode exhibit EDLC nature and showed a good specific capacitance values 94 F/g at the scan rate of 10 mVs^{-1}. From these results,the RGO electrode is ideal candidate for supercapacitor applications.

References

1. Yu, Yang, Chaojiang Niu, Chunhua Han, Kangning Zhao, Jiashen Meng, Xiaoming Xu, Pengfei Zhang, Lei Wang, Yuzhu Wu, and Liqiang Mai. "Zinc pyrovanadate nanoplates embedded in graphene networks with enhanced electrochemical performance." Industrial & Engineering Chemistry Research., vol. 55, no. 11 **(2016)**, pp. 2992-2999.
2. Rakhi, R. B., Wei Chen, Dongkyu Cha, and Husam N. Alshareef. "High performance supercapacitors using metal oxide anchored graphene nanosheet electrodes." Journal of Materials Chemistry., vol. 21, no. 40 **(2011**), pp. 16197-16204.
3. Zaaba, N. I., K. L. Foo, U. Hashim, S. J. Tan, Wei-Wen Liu, and C. H. Voon. "Synthesis of graphene oxide using modified hummers method: solvent influence." Procedia engineering., vol. 184 **(2017)**, pp. 469-477.
4. Emiru, Tarko Fentaw, and Delele Worku Ayele. "Controlled synthesis, characterization and reduction of graphene oxide: A convenient method for large scale production." Egyptian Journal of Basic and Applied Sciences., vol. 4, no. 1 **(2017)**, pp. 74-79.
5. Bose, Saswata, Tapas Kuila, Ananta Kumar Mishra, Nam Hoon Kim, and Joong Hee Lee. "Dual role of glycine as a chemical

functionalizer and a reducing agent in the preparation of graphene: an environmentally friendly method." Journal of Materials Chemistry. vol. 22, no. 19 **(2012**), pp. 9696-9703.

6. Benjwal, Poonam, Manish Kumar, Pankaj Chamoli, and Kamal K. Kar. "Enhanced photocatalytic degradation of methylene blue and adsorption of arsenic (iii) by reduced graphene oxide (rGO)–metal oxide (TiO 2/Fe 3 O 4) based nanocomposites." Rsc Advances., vol. 5, no. 89 **(2015)**, pp. 73249-73260.
7. Naderi, Hamid Reza, Mohammad Reza Ganjali, and Amin Shiralizadeh Dezfuli. "High-performance supercapacitor based on reduced graphene oxide decorated with europium oxide nanoparticles." Journal of Materials Science: Materials in Electronics., vol. 29, no. 4 **(2018),** pp. 3035-3044.
8. Ma, Lina, Ping Zhao, Wenjun Wu, Haijun Niu, Jiwei Cai, Yongfu Lian, Xuduo Bai, and Wen Wang. "RGO functionalised with polyschiff base: multi-chemical sensor for TNT with acidochromic and electrochromic properties." Polymer Chemistry., vol. 4, no. 17 **(2013)**, pp. 4746-4754.
9. Gangwar, Pratisha, Simrjit Singh, and Neeraj Khare. "Study of optical properties of graphene oxide and its derivatives using spectroscopic ellipsometry." Applied Physics A., vol. 124, no. 9 **(2018)**, pp. 1-8.
10. Govindarajan, D., V. Uma Shankar, and R. Gopalakrishnan. "Supercapacitor behavior and characterization of RGO anchored V 2 O 5 nanorods." Journal of Materials Science: Materials in Electronics., vol. 30, no. 17 **(2019)**, pp. 16142-16155.
11. Bhawal, Poushali, Sayan Ganguly, T. K. Chaki, and N. C. Das. "Synthesis and characterization of graphene oxide filled ethylene methyl acrylate hybrid nanocomposites." RSC advances., vol. 6, no. 25 **(2016)**, pp. 20781-20790.
12. Dar, M. A., Govindarajan, D., & Dar, G. N. (2021). Facile synthesis of SnS nanostructures with different morphologies for supercapacitor and dye-sensitized solar cell applications. Journal of Materials Science: Materials in Electronics, 32(15), 20394-20409.
13. Dar, M. A., Bhat, M. Y., Mala, N. A., Rather, H. A., Venkatachalam, S., & Srinivasan, N. (2022). Structural, morphological and supercapacitor applications of SnS nanomaterials prepared in three different types of solvents. Materials Today: Proceedings, 66, 1689-1698.
14. Dar, M. A., Govindarajan, D., & Dar, G. N. (2021). Comparing the electrochemical performance of bare SnS and Cr-doped sns nanoparticles synthesized through solvothermal method. Physics of the Solid State, 63(9), 1343-1350.
15. Dar, M. A., Govindarajan, D., Batoo, K. M., Hadi, M., & Dar, G. N. (2022). Photovoltaic and Supercapacitor performance of SnSe nanoparticles prepared through co-precipitation method. Materials Technology, 37(10), 1396-1409.
16. Dar, M. A., Govindarajan, D., Batoo, K. M., & Siva, C. (2022). Supercapacitor and magnetic properties of Fe doped SnS nanoparticles synthesized through solvothermal method. Journal of Energy Storage, 52, 105034.
17. Mala, N. A., Dar, M. A., Sivakumar, S., Husain, S., & Batoo, K. M. (2022). Enhanced electrochemical properties of zinc and manganese co-doped NiO nanostructures for its high-performance supercapacitor applications. Inorganic Chemistry Communications, 142, 109661.
18. Mala, N. A., Dar, M. A., Sivakumar, S., Husain, S., & Batoo, K. M. (2022). Enhanced

electrochemical properties of zinc and manganese co-doped NiO nanostructures for its high-performance supercapacitor applications. Inorganic Chemistry Communications, 142, 109661.